

UDK 622.785:661.882

## Sintering of Mechanically Activated Magnesium-titanate and Barium-zinc-titanate Ceramics

N. Obradović<sup>1\*)</sup>, S. Filipović<sup>1</sup>, V.B. Pavlović<sup>1</sup>, A. Maričić<sup>2</sup>, N. Mitrović<sup>2</sup>,  
M.M. Ristić<sup>3</sup>,

<sup>1</sup>Institute of Technical Sciences of SASA, Knez-Mihailova 35/IV,  
11000 Belgrade, Serbia

<sup>2</sup>Technical Faculty Čačak, 32000 Čačak, Serbia

<sup>3</sup>Serbian Academy of Sciences and Arts, Knez-Mihailova 35,  
11000 Belgrade, Serbia

---

### **Abstract:**

*In this article the influence of mechanical activation on sintering process of magnesium-titanate and barium-zinc-titanate ceramics has been investigated. Both non-activated and mixtures treated in planetary ball mill for 80 minutes were sintered at 1100°C and 1300°C. The influence of mechanical activation on phase composition and crystal structure has been analyzed by XRD, while the effect of activation and sintering process on microstructure was investigated by scanning electron microscopy. It has been established that temperature of 1100°C was too low to induce final sintering stage for both systems. Moreover, we concluded that barium-zinc-titanate ceramics exhibited better sinterability than magnesium-titanate ceramics.*

**Keywords:** Ceramics; Mechanochemical processing; Sintering; SEM.

---

## 1. Introduction

Development of dielectric binary and ternary materials based on TiO<sub>2</sub> such as barium, strontium and magnesium-titanates, as well as barium-strontium and barium-zinc-titanates is increasing with a rapid progress in mobile and satellite communications systems. These materials can differ extremely low dielectric loss in the microwave range and high dielectric constant [1-3]. Recently barium-zinc-titanate compounds and magnesium-titanate based materials (MgTiO<sub>3</sub> and Mg<sub>2</sub>TiO<sub>4</sub>) have attracted great attention for their specific microwave properties. As a result they can be used as parts of resonators, filters and multilayer ceramic capacitors [4].

These materials are often synthesized by solid state reaction between MgO, TiO<sub>2</sub> and BaCO<sub>3</sub>, ZnO, TiO<sub>2</sub> at relatively high temperatures [5,6]. It has been established that sintering temperature can be lowered down owing to magnesium-titanate and barium-zinc-titanate preparation in nanocrystalline form. In order to produce nanocrystalline powders and improve the final properties of advanced ceramics, among the other methods, high energy mechanical activation can be employed. High-energy ball milling as method for nano size materials synthesis has many advantages, such as simplicity, relatively inexpensive production, applicability to any class of materials, etc [7]. Tribophysical activation is characterized by

---

\*) Corresponding author: obradovic.nina@yahoo.com

crystallite size reduction and increase of dislocation density and lattice strain [8-10]. Moreover, as a result of the reduction in cohesive dispersion domains during activation, the number of defects within the material rises, thus increasing diffusion of oxide's atoms and favoring a solid-state reaction.

Taking all this into account, the influence of mechanical activation of the MgO-TiO<sub>2</sub> and BaCO<sub>3</sub>-ZnO-TiO<sub>2</sub> systems on phase composition, crystal structure and microstructure after sintering process has been reported in this article.

## 2. Experimental procedure

Mixtures of MgO and TiO<sub>2</sub> powders at a molar ratio MgO:TiO<sub>2</sub> = 2:1 were mechanically activated in a high energy planetary ball mill (Retsch type PH 100). Mixtures of BaCO<sub>3</sub>, ZnO and TiO<sub>2</sub> powders at a molar ratio BaCO<sub>3</sub>:ZnO:TiO<sub>2</sub> = 1:2:4 were mechanically activated, also. The milling process of MT and BZT systems was performed in air for 0 and 80 minutes. Ball to powder mixture mass ratio was 20:1. Samples were denoted as MT-0 to MT-80 and BZT-0 to BZT-80, according to the milling time.

The binder-free powders were compacted in an 8 mm diameter tool under 392 MPa pressure. Compacts were placed in an alumina boat and heated in a tube furnace (Lenton Thermal Design Type 1600). MT and BZT compacts were sintered isothermally at 1100 to 1300°C for 2h. The heating rate was 10°C/min. The morphology of obtained powders before and after heating was characterized by scanning electron microscopy (JEOL JSM-6390 LV). The pallets were cracked and covered with gold in order to perform these measurements. X-ray powder diffraction patterns after milling and thermal treatment were obtained using a Philips PW-1050 diffractometer with  $\lambda$ Cu-K $\alpha$  radiation and a step/time scan mode of 0.05°/1s.

## 3. Results and Discussion

The influence of mechanical activation of the MgO-TiO<sub>2</sub> and BaCO<sub>3</sub>-ZnO-TiO<sub>2</sub> systems on phase composition, crystal structure and microstructure has been described previously [11,12]. Main conclusions based upon those investigations are: a mixture of MgTi<sub>2</sub>O<sub>5</sub>, MgTiO<sub>3</sub> and MgO along with very small concentration of TiO<sub>2</sub> phases is observed for the samples activated 80 min, mechanical activation led to particle size reduction and the ratio between final sintering products (MgTiO<sub>3</sub> and Mg<sub>2</sub>TiO<sub>4</sub>) varied with sintering temperature. Simultaneous decrease of TiO<sub>2</sub> anatase, ZnO and BaCO<sub>3</sub> with an increase of BaTiO<sub>3</sub>, ZnTiO<sub>3</sub> and Zn<sub>2</sub>Ti<sub>3</sub>O<sub>8</sub> phases are noticed after 80 min of activation although the dominant phase is a phase of BaTiO<sub>3</sub>. 1100°C is the temperature where one can notice the existence of several phases, such as BaTiO<sub>3</sub>, ZnTiO<sub>3</sub>, Ba<sub>4</sub>ZnTi<sub>11</sub>O<sub>27</sub> and BaZn<sub>2</sub>Ti<sub>4</sub>O<sub>11</sub>.

**Tab. I** Densities of MT-0, MT-80, BZT-0 and BZT-80 before and after sintering process,  $\rho$ (g/cm<sup>3</sup>).

T <sub>s</sub> /milling time	non sintered		1100°C		1300°C	
	0	80	0	80	0	80
MT	1.95 (50.15)	2.36 (60.70)	2.18 (56.10)	2.86 (73.51)	3.15 (80.99)	3.43 (88.30)
BZT	2.70 (55.82)	3.35 (69.26)	3.11 (64.21)	3.81 (78.77)	3.40 (70.25)	4.56 (93.61)

The density of specimens was calculated from precise measurements of specimen's diameter, thickness and mass. Tab. I show densities before and after sintering process. Having in mind greater hardness of MgO, it is clear why the same applied pressure for MT and BZT samples resulted in different pre-sintered densities. Besides, it is obvious that mechanical activation led to better compactness of non sintered samples. Comparing density's values for sintered one, it can be noticed greatest densification for MT-80 and BZT-80 sintered at 1300°C. Also, the greatest density liken theoretical density show specimen BZT-80. It is in accordance with SEM analyses, where we established better sinterability of BZT than MT ceramics.

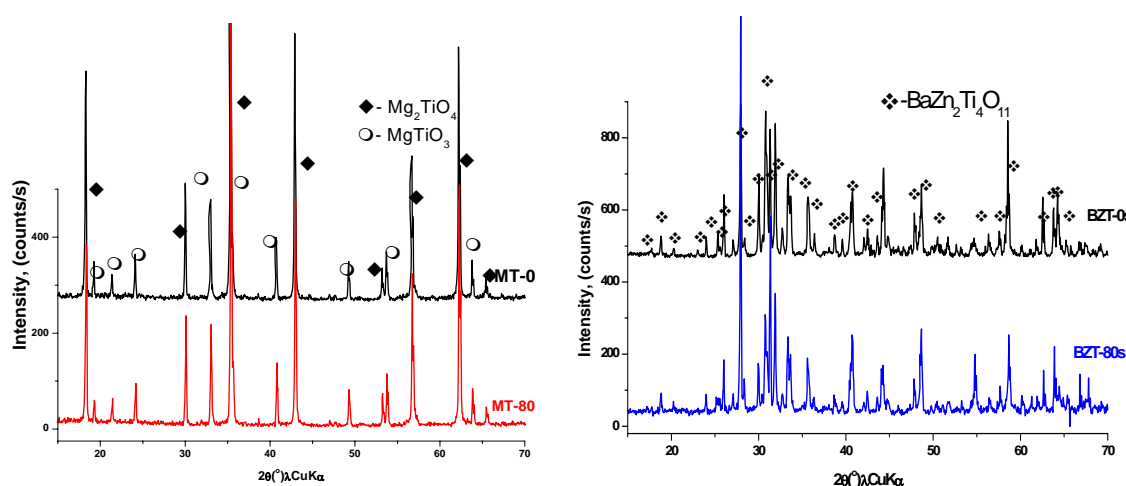


**Fig. 1.** XRD patterns of (a) MT-0 and MT-80, (b) BZT-0 and BZT-80 sintered at 1300°C for 2h.

Fig. 1. (a) presents X-ray diffraction patterns for MT-0 and MT-80 sintered at 1300°C for 2h. The identification of all obtained reflections has been accomplished using the JCPDS card (73-1723 for  $\text{Mg}_2\text{TiO}_4$  and 79-0831 for  $\text{MgTiO}_3$ ). As we can see, both samples consist of two phases, small amount of  $\text{MgTiO}_3$  perovskite phase, together with the dominant  $\text{Mg}_2\text{TiO}_4$  spinel phase. X-ray diffraction patterns of sintered BZT-0 and BZT-80 samples are given in Fig. 1. (b). The identification of all obtained reflections has been accomplished using the JCPDS card (81-2380 for  $\text{BaZn}_2\text{Ti}_4\text{O}_{11}$ ). Only a pure barium–zinc–titanate phase is obtained within both samples and the obtained reflections are sharp and intensive, revealing their crystal structure.

Microstructure parameter, average particle size ( $D_{hkl}$ ), calculated from an approximation method [13] applied on sintered powder mixtures, are given in Tab. II. These calculations have been conducted for the most intensive reflections of  $\text{Mg}_2\text{TiO}_4$ ,  $\text{MgTiO}_3$  and  $\text{BaZn}_2\text{Ti}_4\text{O}_{11}$ . Some of the calculations were not possible to conduct due to great peak broadening and overlapping with some reflections of the final products. It is well known that processes of grain growth, defect disappearance and recrystallization occurred during sintering. Analyses of microstructure parameters calculated from the XRD data indicate that the grain growth with the increasing sintering temperature is present for BZT samples. In the case of MT-80, mechanical activation resulted in non-linear grain growth at higher sintering temperature, which is a desirable property for electrical measurements.

**Tab. II** Microstructure parameters revealed from an approximation method,  $D_{hkl}$  (nm).

sample	phase	1100°C			1300°C		
		(411)	(232)	(223)	(411)	(232)	(223)
<b>BZT-0</b>	BaZn <sub>2</sub> Ti <sub>4</sub> O <sub>11</sub>	19.07	46.53	46.73	75.23	84.87	60.37
<b>BZT-80</b>	BaZn <sub>2</sub> Ti <sub>4</sub> O <sub>11</sub>	11.16	35.10	48.29	142.98	89.94	120.80

sample	phase	1100°C			1300°C		
		(111)	(220)	(400)	(111)	(220)	(400)
<b>MT-0</b>	Mg <sub>2</sub> TiO <sub>4</sub>			75.30	90.69	92.69	113.47
<b>MT-80</b>	Mg <sub>2</sub> TiO <sub>4</sub>	84.10	123.85	76.80	72.09	104.87	76.49

sample	phase	1100°C			1300°C		
		(012)	(104)	(024)	(012)	(104)	(024)
<b>MT-0</b>	MgTiO <sub>3</sub>	93.30	86.10	83.40	90.96	86.67	128.29
<b>MT-80</b>	MgTiO <sub>3</sub>	92.10	112.20	90.80	90.98	92.79	78.30

Micrograph of MT-0 sintered at 1100°C for 2h is given in Fig. 2. (a). It was noticed a formation of contact necks at the beginning stadium of sintering process.

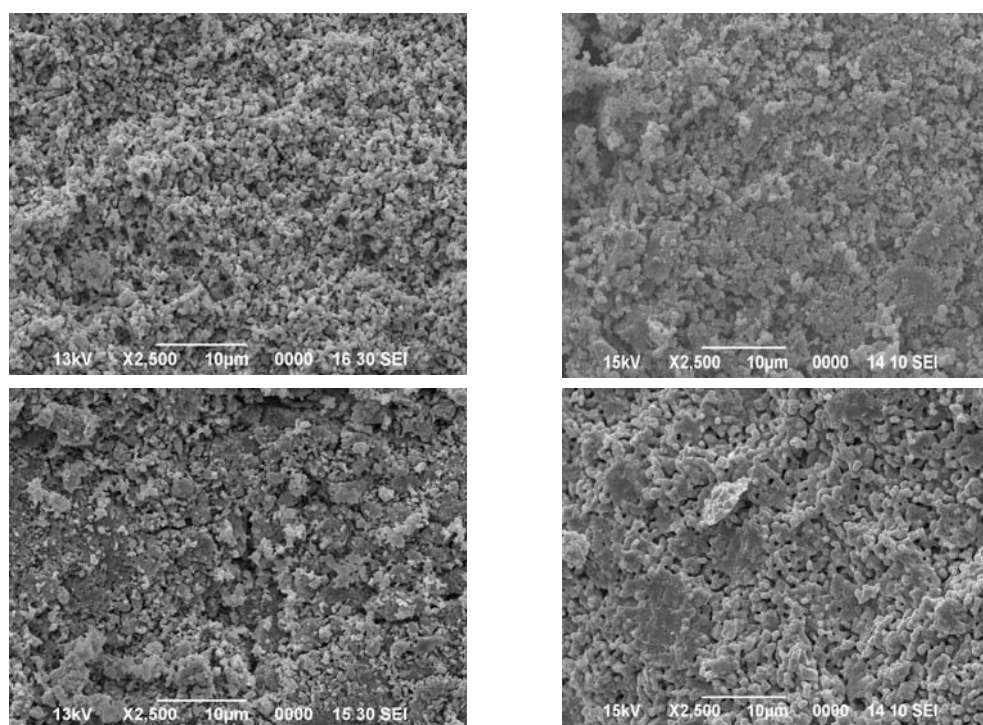


**Fig. 2.** SEM micrographs of (a) MT-0, (b) BZT-0, (c) MT-80 and (d) BZT-80 sintered at 1100°C for 2h.

Grains possess their starting shape and no relevant mass transport has been observed. Fig. 2. (b) shows BZT-0 sintered at 1100°C for 2h. Insufficiently sintered sample and formation of contact necks are the main characteristics for BZT-0, along with small particles of various compounds within the starting sintering phase. At Fig. 2. (c) is clearly visible a formation of new phases along with densification of that segment. It can be also distinguished

appearance of large pores between these grains of new phases and smaller grains of MgO and TiO<sub>2</sub>. Micrograph of sample BZT-80 sintered at same condition is presented at Fig. 2. (d). The initial stage of sintering is still present and grains have polygonal shape. Formation of enclosed pores and presence of two different phases (ZnTiO<sub>3</sub> and BaZn<sub>2</sub>Ti<sub>4</sub>O<sub>11</sub> that are confirmed by X-ray analyses [9]) are almost homogenous arranged. In addition, it can be noticed much denser sample, so it was assumed that dominated process is densification against reaction sintering.

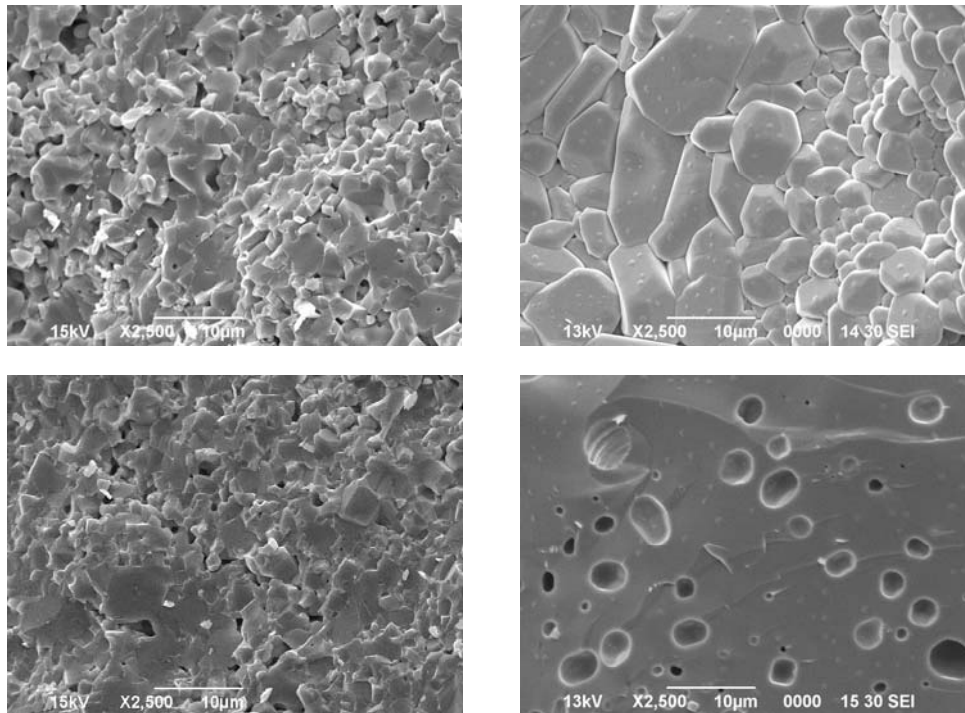


**Fig. 3.** SEM micrographs of (a) MT-0, (b) BZT-0, (c) MT-80 and (d) BZT-80 sintered at 1300°C for 2h.

Fig. 3. shows micrographs of samples sintered at 1300°C for 2h. Medium sintering stages along with enclosed pores are visible for sample MT-0. Presence of two different phases MgTiO<sub>3</sub> and Mg<sub>2</sub>TiO<sub>4</sub> is observed. Smaller grains with polygonal shape (MgTiO<sub>3</sub>), qualify fracture between the grains, while more compact area of Mg<sub>2</sub>TiO<sub>4</sub> qualifies fracture through the grains. Microstructural analysis for BZT-0 sample (Fig. 3. (b)) showed non-uniform grain growth along with grains greater than 20 microns. As a result of reaction sintering process, existence of large pores has been noticed as well.

Formation of enclosed not spherical pores for sample MT-80 (Fig. 3. (c)), is indication of medium sintering phase. More compact sample and presence of fracture between grains, which is probably due to presence of agglomerates in starting powders [11], were essential features of this sample. Two different phases were present, also. Fig. 3. (d) shows micrographs of BZT-80 sintered at 1300°C for 2h. The most homogenous microstructure was obtained. Namely, pure barium–zinc–titanate phase is obtained as well as spherical and enclosed pores, 2 microns in size approximately, which is a sign of final stadium of sintering process.

#### 4. Conclusion

In this paper influence of mechanical activation on sintering of MgO-TiO<sub>2</sub> and BaCO<sub>3</sub>-ZnO-TiO<sub>2</sub> systems were investigated. Comparing density's values, it was found that the greatest densification has been achieved after milling process at highest sintering temperatures. It was concluded that temperature of 1100°C was too low to induce final sintering stage for both systems. Several different phases were noticed along with large pores and small grains.

Formation of various magnesium-titanate phases and pure barium-zinc-titanate phase along with densification process is observed during micrographs analysis for samples sintered at 1300°C. The pure spinel phase Mg<sub>2</sub>TiO<sub>4</sub> is not possible to obtain using these conditions, as a consequence of the thermodynamic instability of spinel phase [6]. One can notice that MT samples activated 80 minutes have lower density than BZT samples which were activated for the same time, also microstructural analyses indicated it is a medium sintering stage for MT-80 and final stadium for BZT-80. As we know, MgO is very rigid and stable oxide and therefore obstructs mechanical treatment, mechanochemical reaction and sintering process [14]. Finally, presented SEM and X-ray analyses of these samples showed advantageous microstructures, with the appropriate pores/materials ratio and good candidates for application in electronic industry.

#### Acknowledgements

This study was supported by the Ministry of Science of the Republic of Serbia (Project 172057 and projects F-7 and F/198 supported by Serbian Academy of Sciences and Arts).

#### 5. References

1. G. Pfaff, *Ceram. Inter.*, 20 (1994) 111.
2. H. Kang, L. Wang, D. Xue, K. Li, C. Liu, *J. Alloys Compd.*, 460 (2008) 160.
3. A. Belous, O. Ovchar, D. Durylin, M. Valant, M. Macek-Krzmanac, D. Suvorov, *J. Eur. Ceram. Soc.*, 27 (2007) 2963.
4. W. Guoqing, W. Shunhua, S. Hao, *Mat. Lett.*, 59, (2005) 2229.
5. A. Balous, O. Ovchar, M. Macek-Krzmanac, M. Valant, *J. Eur. Ceram. Soc.*, 26, (2006) 3733.
6. N. Stubicar, A. Tonjevic, M. Stubicar, *J. Alloys Compd.*, 370, (2004) 296.
7. K. T. Paul, S. K. Satpathy, I. Manna, K. K. Chakraborty, G. B. Nando, *Nanoscale Res. Lett.*, 2 (2007) 397.
8. M. G. Kakazey, L. A. Klockov, I. I. Timofeeva, T. V. Srećković, B. A. Marinković, M. M. Ristić, *Cryst. Res. Technol.*, 34 (1999) 859-866.
9. M. G. Kakazey, V. A. Melnikova, T. V. Srećković, T. V. Tomila, M. M. Ristić, *J. Mat. Sci.*, 34 (1999) 1691-1697.
10. N. Obradović, N. Labus, T. Srećković, M. M. Ristić, *Mat. Sci. Forum*, 518 (2006) 131-136.
11. S. Filipovic, N. Obradovic, V. B. Pavlovic, S. Markovic, M. Mitric, M. M. Ristic, *Sci. Sint.*, 42, (2010) 143.
12. N. Obradovic, S. Filipovic, V. Pavlovic, M. Mitric, S. Markovic, V. Mitic, N. Djordjevic, M. M. Ristic, *Ceram. Int.*, (2010), doi:10.1016/j.ceramint.2010.07.001.
13. Lj. Karanović, *Applied crystallography* (Belgrade University, Belgrade 1996) 91 (in Serbian).

- 
14. N. Obradovic, S. Stevanovic, M. M. Ristic, *Powd. Met. and Met. Cer.*, 47, (2008) 63.

---

**Садржај:** У овом раду проучаван је утицај механичке активације магнезијум-титаната и баријум-цинк-титаната на њихово синтеровање. И неактивирани смеша и смеше активирани 80 минута у планетарном млину синтеровани су на 1100 и 1300°C. Утицај механичке активације на фазни састав и кристалну структуру проучаван је рендгенском дифракцијом, док је ефекат активације, заједно са процесом синтеровања, праћен скенирајућом електронском микроскопијом. Установљено је да је температура од 1100°C ниска да би довела оба система до завршног стадијума синтеровања. Даље, закључили смо да баријум-цинк-титанатна керамика показује бољу синтерабилност у односу на магнезијум титанатну.

**Кључне речи:** Керамика; механичка активација; синтеровање; скенирајућа електронска микроскопија.

---